



Numerical investigation of free natural convection in an open vertical channel with asymmetric heating

Sarra Fatnassi^{1,2}, Aissa Abidi-Saad^{3,4}, Rejeb Ben Maad¹, Guillaume Polidori²

¹Laboratory of Energizing and Thermal and Mass Transfers, University of Tunis El Manar, Tunis, Tunisia

² Research Group in Engineering Sciences (GRESPI EA4694), University of Reims, 51100 Reims, France

³Laboratory of Applied Energetic and Pollution, Constantine University 1, Constantine 25000, Algeria.

⁴University kasdi Merbah, Ouargla 30000, Algeria.

sara-fatnassi@hotmail.com¹

asais83@yahoo.fr^{3,4}

benmaadrejeb@gmail.com¹

guillaume.polidori@univ-reims.fr²

Abstract:

A numerical study in an open-ended vertical channel is carried out in order to describe the fluid dynamics and heat transfer of free convection inside a vertical channel asymmetrically heated at uniform heat flux. Non-uniform heating configurations in which heat sources alternated with unheated zones on one/both walls were studied to simulate opaque PV arrays and glazed panes/windows of the building. The numerical simulations were performed in water for an aspect ratio of the vertical channel (ratio between channel width and height of heated zone) equal to 5.2 for the reference case, then it changes as the length of the heated zone changed. Finite volume based commercial software ANSYS 15.0 (Fluent) is used to solve the governing equations. The investigations focused more specifically on the influence of the length, number and alternation of the heated zones inside the channel in steady-state regime on the flow structure and heat transfer performance. The numerical results showed that, the effect of heat sources distribution has a strong impact on the flow structure. The analysis of the Nusselt number and parietal temperature profiles clearly indicates that the convective heat transfer can be enhanced or reduced with the heat source alterations.

Keywords: Natural convection, CFD, vertical channel, asymmetric heating, heat source alterations.

1. Introduction

The energy issue in the building sector is one of the major challenges of sustainable development. This sector is one of the biggest consumers of energy today. Therefore, it is among the largest producers of Greenhouse gas (GHG). The reduction of GHG emissions revolves around three main axes which are: saving energy, improving

the energetic efficiency of some systems and finally the production of electricity from a local renewable energy. the latter perspectives have one of the most effective solutions which is the large-scale integration of PV panels on building façades and/or roofs, creating vertical and/or inclined double skin façades (DSF). That means, the PV panels can be used in the building sector due to the large surface offered by the building envelope (BIPV), where they can be alternated with glazing windows.

Nomenclature			
A	heated length, m	u,v	vertical and transversal velocity components, m/s
b	channel wall spacing, m	x,y	vertical and transversal coordinates, m
C_p	specific heat capacity, J/kg.K	Greek symbols	
g	acceleration of gravity, m/s^2	β	volume expansion coefficient
k	thermal conductivity, W/m.K	ϕ	heat flux density, W/m^2
H	channel length, m	T	temperature, K
S	spacing between heat zones, m	ρ	density, Kg/m^3
Nu_{ave}	averaged Nusselt number, $(Nu_{ave}=\bar{h}\times 2A/k)$	ν	kinematic viscosity, m^2/s
P	pressure, Pa	μ	dynamic viscosity, Pa.s
Pr	Prandtl number ($Pr=\nu/a$)	Indices	
Ra	Rayleigh number ($Ra=(g\beta\phi b^4)\times Pr/k\nu^2$)	W	wall
Ra^*	modified Rayleigh number ($Ra^*=Ra/R_f$)	0	reference value
R_f	aspect ratio ($R_f=A/b$)		

In literature, the double skin façade and PV panels were modeled by a vertical/inclined asymmetrically heated channel in several works, in order to understand the flow and heat transfer in these systems. It is crucial to gain a deeper knowledge and understanding of both dynamic and thermal behaviors of such systems. Since PV panels are a renewable energy sources to produce electricity. The portion of the solar energy that is converted by PV panels into electricity is in the range of 18–20% [17], due to an internal temperature rise of the PV panel, which is responsible of a decrease in both the electrical conversion efficiency and reliability.

The modeling of the natural convection flow and deduced convective heat transfer exchange in such geometry remains a difficult problem to be solved, especially due to the difficulty of defining of the suitable boundary conditions at the inlet and outlet interfaces of the channel. It still a largely open question in literature since the full form of the conservation equations is limited to the single channel geometry. The work of Elenbaas in 1942 [5] is the first in this field. In his work two flow dynamic regimes within a vertical channel were observed. The appearance of these regimes depends on the modified Rayleigh number (Ra^*). Indeed, for a relatively low Rayleigh number the author finds a fully developed regime. However, for high Rayleigh number, a boundary layer is observed near the heated wall; the fluid simultaneously enters from below and exits through the top of the channel via a reversed flow observed near the unheated wall. Fohanno et al [7] and Ospir et al [8] characterized the flow structure induced by natural convection in vertical channel asymmetrically heated using water as working fluid. Their results indicated an upward flow accompanied by a downward cold fluid in the form of big recirculation zone in the channel outlet. Subsequently, another study was carried out by Ospir et al in 2012 [9] for the same configuration but for various modified Raleigh numbers (Ra_b^*) varying between 4.5×10^5 and 4.5×10^6 . Flow visualizations (streamlines) were presented for different time steps. They highlighted a recirculation zone along the adiabatic wall located at the center of the channel. Their results showed that the length of recirculation tends to decrease with the increase of Ra_b^* . But, for a fixed Ra_b^* , the total length of the recirculation zone is more important for the small aspect ratio. Similarly, Popa et al [10] showed that the length of the recirculation zone gradually decreases with the increase in both: the aspect ratio of the channel and the modified Rayleigh number. Frédéric et al. [11] explored natural convection air flow in a vertical channel heated by a constant heat flux density on the left wall. The heat flux ranges from $q = 10 W/m^2$ to $q = 75 W/m^2$ correspond to a Rayleigh number ranging from 6×10^9 to 4.5×10^{10} . The authors have defined three classes of reverse flows according to an analysis of the velocity histogram: absence, intermittence and permanence.

Since the phenomenon of reverse flow is not well understood still nowadays, the work of Polidori et al [12] focuses only on the early stage of the development of the flow within a channel. The analysis of streamlines indicates the creation of two cells (C1 and C2). Consecutively, a beating was noticed from the right to the left of the viscous layer. This beating caused an inverse principal flow coming from the imbalance of the pressure at the end of the channel.

On the other hand, the natural convection in the inclined channels has been widely studied. Among the experiments in natural convection on an inclined channel is the study conducted by Imran et al [13], to predict its performance under varying geometrical features. The flow inside the chimney was investigated numerically for inclination angles varying from 15 to 60, solar heat flux 150-750 W/m² and for chimney thickness 50, 100 and 150 mm. The numerical results showed that the velocity increases continuously with the increase in the inclination angle and solar heat fluxes and decreases with increases of chimney thickness. Also, their results indicated that; the optimum chimney inclination angle was 60 to obtain the maximum rate of ventilation. Also, Hemmer et al. [14] investigated the heat transfer and flow dynamics in inclined PV panels. Irrespective of the inclination, they found a reversed flow at the channel outlet. The inclination angle has a weak influence on the flow structure and heat transfer. Moreover, the maximal heat transfer rate is found for the inclination angle $\Theta=0$.

For the case of enhancing and controlling the flow and heat transfer, among others works, Abidi-saad et al have carried out two investigations, numerical [18] and experimental [19]. They concentrated on the effect of the size and position of two symmetrically attached ribs inside an asymmetrically heated channel. In their numerical work, an optimal ribs size is found which enhance both heat transfer and mass flow rate. Their findings are suitable for “hybrid” solar applications (photovoltaic/thermal, PV/T solar collectors) where the electricity produced by PV panels can be associated to the heating and cooling duties of building (heat recovery and ventilation). Besides that, in their experimental study, the best position of the two ribs for heat transfer enhancement is that when they attached in the top of the heated zone. Also, in the both works a reversed flow is noticed.

To study the influence of the heat source distribution, Hemmer et al. [15] studied the case of a non-uniformly heated channel for three numbers of modified Rayleigh. Their results showed that the convective heat transfer increases with the dissipated power. Also, the mass flow rate calculated at the bottom of the channel is always important whatever is the dissipated power. For the other configurations, the outer skin is composed of alternating PV modules (heat sources) and glazed panes (unheated zones) over its entire height. The effects of the non-uniformity of the wall heat flux distribution on the natural convection flow and heat transfer within a vertical channel has been studied by Tkachenko et al. [16]. Their finding shown that the alternation of the heated and unheated zones leads simultaneously to the enhancement of convective heat transfer (lower wall temperature) and to an increase of the chimney effect (induced mass flow rate).

As stated previously, there is still a lack of fundamental knowledge and well comprehension of the main dynamic and thermal behaviors of DSF and PV panels, which is the key in designing panels that maximize efficiency and minimize energy losses. In this paper, a dynamical study of the flow in a vertical asymmetrically heated channel, a prototype of double-skin façade, is carried out numerically. The channel was immersed in a tank filled with water corresponding to the domain of study, to overcome the difficulty in defining the pressure boundary conditions at inlet and outlet of the channel. The use of water as working fluid is to neglect the thermal radiation. The aim of this study is to examine the influence of the length of the heat sources distributed on one of the two walls of the channel. Also, the effect of the spacing between the heat sources and the alternation of the heated zones with the adiabatic zones was examined.

2. Channel description:

The global geometrical configuration (reference case) is the same of that used in previous works [1] [2]. The vertical channel is made up of two parallel plates of height H ($H = 376$ mm) separated by a distance $b = 36$ mm. The channel aspect ratio is $R_f = A/b$, and the Prandtl number of the working fluid Pr is 7. The reference case (called case 0) considered here is composed of a heated central part whose height is $A = H/2=188$ mm completed with two adiabatic unheated extensions (length $A/2$) respectively located at the bottom

and top open ends of the channel, while the opposite wall remains entirely unheated throughout the duration of the simulations (Fig. 1). In addition, for a better control of the flow conditions at the entrance, a quarter circle ($R = 36\text{mm}$) was added at the bottom of each wall. The channel is immersed in a vertical tank ($500 \times 500 \times 1000 \text{ mm}^3$) made up of 20 mm thick Plexiglas plates and filled with water which allows to overcome the pressure boundary conditions at inlet and outlet of the channel (Desrayaud et al. [6]). The choice of water as working fluid leads to a negligible effect of heat transfer by radiation. Moreover, in this numerical study the conduction in the heating wall is not taken into account since Ospir et al [1] experimentally observed no influence of the axial conduction for the same channel/environment geometry.

To study the influence of the distribution of the heated zones, many possibilities of heat sources alteration were made. Firstly, the length of the heated zone is increased, which is set equal to that of the length of the channel (Fig.2; case 1). In the second case, the length of the heated zone was decreased to half of that of the reference case. For the third case, the heated area of case 2 is divided into two identical spaced heat sources. The height of the spacing (S) and each heat source is $A/2$ and $A/4$ respectively. Both heat sources were heated by means of the same heat flux density. In the last case the heat sources alternation changes between the two walls of the channel as presented in (Fig. 2; case 4) showing several heat sources numbers and arrangements. The lengths of the heated and the unheated areas are identical and equal to $A/2$.

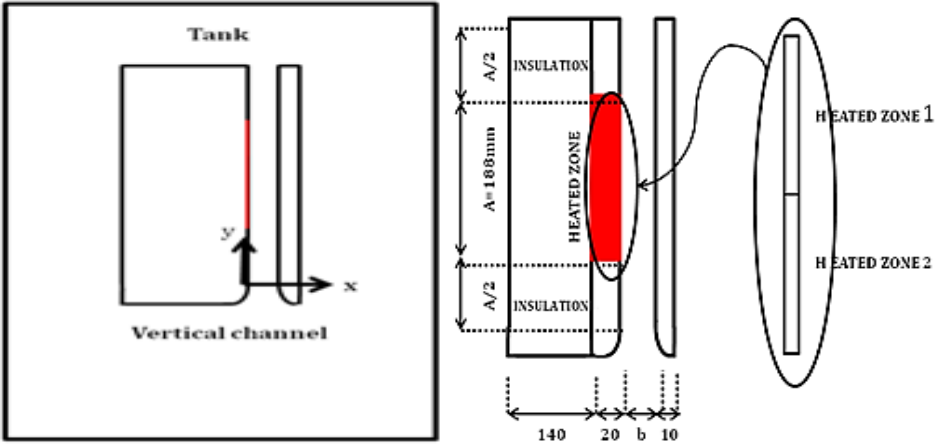


Figure 1: Geometry setup: computational domain (left) and sketch of the channel case 0 (right).

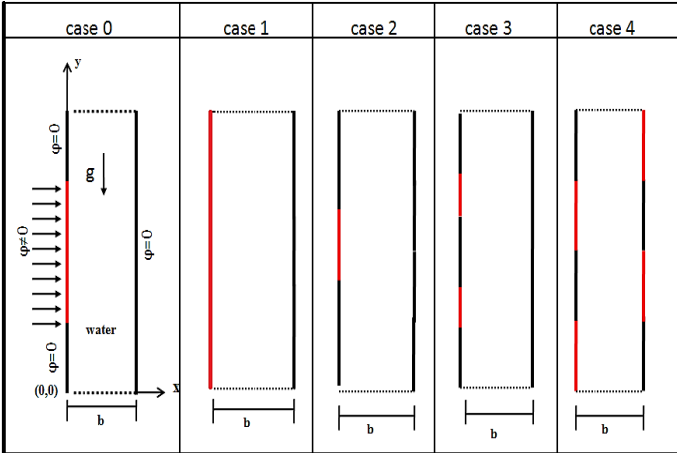


Figure 2: The different geometries studied

3. Physical setup:

The natural convection generated by heat transfer in the vicinity of the heated surfaces has been widely studied theoretically and experimentally. The numerical simulations of the channel flow are carried out for two-dimensional steady laminar flow. In the laminar case, fluid flow and heat transfer problems can be solved by the resolution of continuity, momentum and energy equations. These three equations are solved numerically using the finite volume method [3]. In this study the flow is considered as laminar, unsteady, and two-dimensional [4]. The fluid is Newtonian, incompressible, and the physical properties (ρ, C_p, k, μ) of the fluid are temperature dependent. The channel is initially immersed in a tank filled with water whose temperature is $T = 288$ K. In this problem all thermophysical properties of the fluid are defined as functions of temperature [4]. The used polynomial temperature dependent formulae are given in Abidi-Saad et al [18].

With all the assumptions mentioned above, the dimensionless unsteady-state conservation equations are as follows:

- Continuity equation:

$$\frac{\partial U}{\partial X} + \frac{\partial V}{\partial Y} = 0 \quad (1)$$

- Momentum equations:

$$\frac{\partial U}{\partial t} + \frac{\partial(U^2)}{\partial X} + \frac{\partial(UV)}{\partial Y} = -\frac{\partial P}{\partial X} + Pr \left(\frac{\partial^2 U}{\partial X^2} + \frac{\partial^2 U}{\partial Y^2} \right) \quad (2)$$

$$\frac{1}{R_f} \left(\frac{\partial V}{\partial t} + \frac{\partial(UV)}{\partial X} + \frac{\partial(V^2)}{\partial Y} \right) = \frac{1}{R_f} \left(-\frac{\partial P}{\partial Y} + Pr \left(\frac{\partial^2 V}{\partial X^2} + \frac{\partial^2 V}{\partial Y^2} \right) \right) + Ra^* Pr \theta \quad (3)$$

- Energy equation:

$$\frac{\partial \theta}{\partial t} + \frac{\partial(U\theta)}{\partial X} + \frac{\partial(V\theta)}{\partial Y} = \left(\frac{\partial^2 \theta}{\partial X^2} + \frac{\partial^2 \theta}{\partial Y^2} \right) \quad (4)$$

Equations (1)–(4) have been obtained from their dimensional counterparts by using the following dimensionless:

$$X = \frac{x}{b}; Y = \frac{y}{b}; U = \frac{ub}{\alpha}; V = \frac{vb}{\alpha}; P = \frac{(p + \rho g y)b^2}{\vartheta \alpha^2}; \alpha = \frac{k}{\rho c_p}; \theta = \frac{(T - T_0)k}{\varphi b}$$

The dimensionless analysis leads to three other dimensionless quantities appearing in the governing equations.

- The aspect ratio (R_f) which is a characteristic of the channel geometry:

$$R_f = \frac{A}{b} \quad (5)$$

- The modified Rayleigh number (R_a^*) defined as:

$$R_a^* = \frac{Ra}{R_f} = \frac{g\beta\varphi b^4}{k\nu^2} \frac{b}{A} Pr \quad (6)$$

Where β , ν , α are the thermal expansion coefficient, the kinematic viscosity and the thermal diffusivity, respectively.

The problem depends on several physical parameters: the aspect ratio of the heated zone R_f and the modified Rayleigh number Ra^* , as introduced by Elenbaas [5]. The velocity and temperature boundary conditions used in this problem (Figure 2, case 0) are chosen as follows.

- On the right wall (adiabatic wall of case 0) $X=1$ and $0 \leq Y \leq 2R_f$

$$U=V=0; \varphi=0$$

- On the left wall (heated wall of case 0) For $X=0$ and $0 \leq Y \leq R_f/2$, $3R_f/2 \leq Y \leq 2R_f$

$$U=V=0; \varphi=0$$

$$\text{For } X=0 \text{ and } R_f/2 \leq Y \leq 3R_f/2$$

$$U=V=0; \varphi > 0$$

Once the flow and thermal fields are computed, the surface averaged Nusselt number was calculated at the hot wall (case 0) using the formula:

$$Nu_{ave} = \frac{\bar{h}}{k} A = \frac{1}{A} \left[\int_{A/2}^{3A/2} \frac{\varphi}{k(T_w - T_0)} dy \right] \quad (7)$$

4. Numerical method and code validation:

The mass, momentum and energy conservation equations have been solved numerically using a finite volume method [3]. This method is based on the spatial integration of transport equations in elementary volumes. The coupling between velocity and pressure is achieved with the algorithm Coupled Scheme that solves the equations of continuity and momentum simultaneously, which gives an advantage to treat flows with a strong interdependence between dynamic and thermal fields.

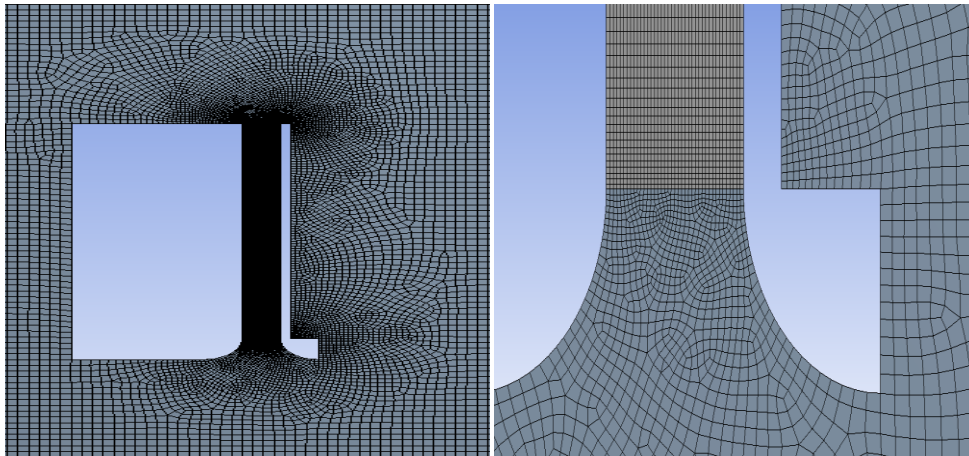


Figure 3: Meshing

Numerical simulations are performed with the commercial software ANSYS Fluent CFD. The mesh of the fluid domain is, on the one hand, structured inside the channel ($\Delta y = 3.9$ mm; $\Delta x = 0.9$ mm). On the other hand, unstructured and progressive outward from the tank. The grid independence study has been performed to ensure that the solution is independent on the mesh size. The total number of cells in the whole calculation domain is

found equal to 28,000 (Fig. 3). The convergence criteria were based on the residuals resulting from the integration of the conservation equations (1) – (4) over finite control volumes. During the iterative calculation process, these residuals were constantly monitored and carefully scrutinized. For all simulations performed in this study, converged solutions were achieved with residuals as low as 10^{-4} (or less) for all the governing equations.

The validation of our numerical results is achieved by comparing the present temperature differences in the vicinity of the heated wall for the reference case (case 0) with experimental data of Polidori et al [12]. It is presented in Abidi-Saad et al [18] and it is not necessary to be repeated here.

5. Results and discussion

Both convective heat transfer and flow dynamics in asymmetrically heated channel, representative of PV panel, double skin facades and BIPV applications, are investigated numerically. The thermal radiation has been voluntarily omitted by using water as working fluid. The study has focused on the effect of the length, number and alternation of the heat sources on heat transfer and flow dynamics. The study is carried out for a modified Rayleigh number $Ra^* = 4.5 \times 10^6$ based on a fixed aspect ratio of the heated part ($R_f = A/b = 5.2$ for case 0). Also, the modified Rayleigh number based on the heat flux density ($\phi = 510 \text{ W/m}^2$ which represents the average solar flux over a year in France) and the width of the channel (b). Concerning the value of the heated part aspect ratios R_f , it is within the range of those found for horizontally divided double-skin facades of high-rise buildings [10]. The calculations were first started in a transient mode from $t = 0$ by heating the fluid up to $t = 30 \text{ mn}$. The results are presented in the steady state regime, which was considered achieved from $t = 30 \text{ mn}$ (Ospir et al [9]).

5.1 Flow structure

Fig. 4 (a – e) shows the numerically obtained streamlines patterns at $t = 30 \text{ mn}$ for the reference case (Fig. 4a) and the other cases. From the cases 0-3, it can be seen, an ascending boundary-layer flow develops near the heated wall due to the feeding of fluid from the bottom of the channel. At the same time, cold fluid enters the channel from its top-end, near the unheated right wall and supplies a reverse flow developing near the unheated right wall. This appearance of the reverse flow in the upper half of the channel is due to the fact that, the lateral feeding of the boundary layer is prevented by the lateral confinement of the open-ended plane channel, which causes large-scale flow instabilities. Besides that, it is due to the insufficient feeding of the boundary layer flow from the bottom of the channel. The length of the reverse flow depends on the length of the heated zone. It is almost equal to that of the heated zone for the reference case 0, case 2 and case 3. For the case 1 it is equal to three quarter of the channel height with the appearance of another small vortex attached to the unheated wall in the exit of the channel. Fig. 4e, presents the streamlines plots for the case 4 where the heated part on the left wall (of case 0) is divided into two heat sources separated by an adiabatic spacing ($s = A/2$). On the other hand, on the opposite wall two heat sources are added with alternation to those of the left wall. It is noticed that, the supplementary heat sources on the adiabatic right wall affect considerably the flow structure. In fact, these heat sources act as a supplementary motor of the ascending fluid motion. Due to this fact, another boundary layer flow type is created in the vicinity of the added heat sources on the right wall which shifts the reversed flow to the channel centerline. Whereas, streamlines become quasi-parallel to the channel left wall. Only a little bias is observed in the vicinity of this wall exactly in the channel inlet. Moreover, a wavy pattern of streamlines is found in the central part of the channel (channel centerline). Also, the reverse flow is almost totally ejected from the channel, only its head remains in the channel exit. That is due to the fact that a strong adverse pressure applied by the two upward flows on the reverse flow that blocks the channel exit. But, it remains insufficient to eject all the reverse flow out of the channel.

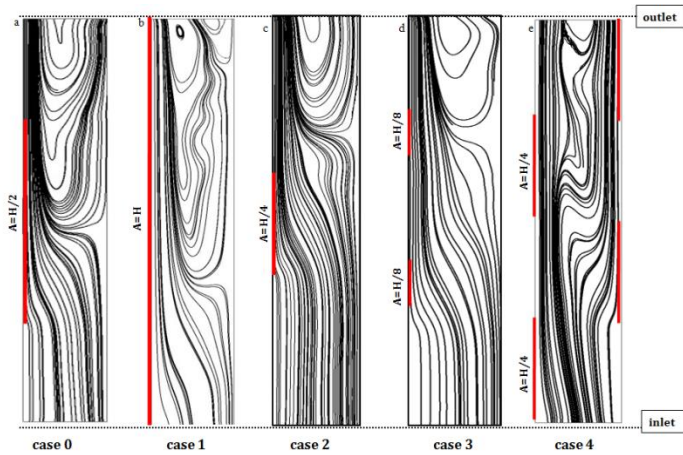


Figure 4: The different geometries studied

5.2 Velocity profiles

Figures 5 and 6 show the vertical velocity profiles at the channel inlet and outlet respectively. From Fig. 5 it can be seen that the velocity profiles are approaching the laminar flow profiles for the cases 0, 1, 2 and 3. Whereas, for the case 4 the velocity profile is disfigured, resulting in curves with two peaks (two maxima). The maximum velocity near the left and right walls is 2.3 and 1.9 mm/s, respectively. This fact can be conceived as two separate jets adjacent to the partially heated walls. The highest velocity magnitude is found for the case 4 compared to all studied cases. Then; the case 1, where the left wall is entirely heated.

From Figure 6 for the cases 0, 1, 2 and 3, as soon as the fluid enters the heated section, the velocity profile exhibits a boundary layer structure, with a strong acceleration in the vicinity of the heated left wall. Due to the fact that the fluid undergoes a high buoyancy force near the heated zone. The strength of the velocity depends on the length of the heated part. Negative velocities are noticed near the adiabatic right wall for all cases indicating the reverse flow. For the case 4 where the four heated zones are alternated on both channel walls, a hydrodynamic boundary layer develops along the both walls of the channel. Velocity near the channel walls increases with increasing axial location, showing two maxima 5.023 and 4.548 mm/s near the left and the right walls respectively.

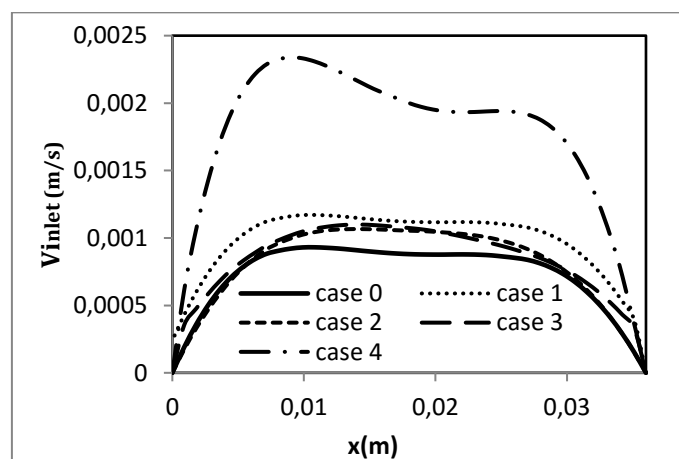


Figure 5: Axial velocity profiles for $Ra^*=4.5 \times 10^6$ at the entrance of the channel

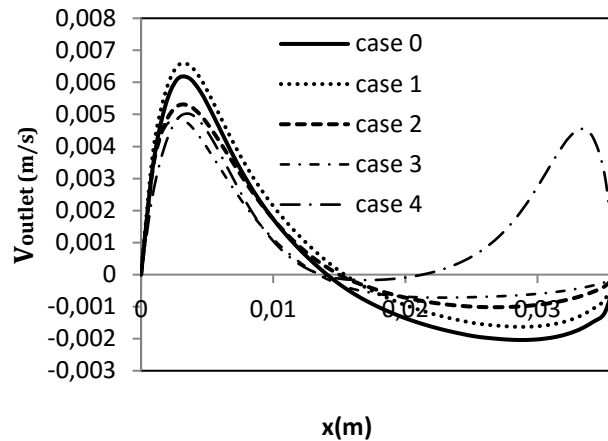


Figure 6: Axial velocity profiles for $Ra^*=4.5 \times 10^6$ at the outlet of the channel

5.3 Heat transfer

Figure 7 displays the comparison of temperature difference profiles along the heated sections of the left wall of the channel for all cases. For the cases 3 and 4 temperature profiles are found to oscillate periodically with the alternation of heated and unheated zones. Indeed, for all cases the surface temperature on the left wall increases sharply in the heated zones, from the minimum value at the leading edge to the maximum one at the trailing edge, and decreases along the unheated zones. The important finding is that the lowest average temperature is found for the case 3. This result indicates that the maximum heat transfer rate characterized by heat transfer coefficient $h = \phi / (T_w - T_0)$ is found for case 3. These findings are confirmed in Figure 8 which presents the average Nusselt number plots for all studied cases. As it can be seen from Figure 8 the largest heat transfer rate is found for case 3 then for case 2. It could be due to the reason that at these two cases the reverse flow is very small compared to the reference case (see Fig. 4, Cases 2, 3). Which allows a large space for the incoming fluid (significant quantity of the fluid coming from the bottom of the channel). The average heat transfer rates for the cases 1 and 4 are the smallest compared to that of the reference case (case 0). Due to the blocking of the $\frac{3}{4}$ of the channel length by the reverse flow for the case 1 (Fig. 4, case 1). But for the case 4, despite to the quasi-complete ejection of the reversed flow, the decrease of the Nu_{ave} is due to the division of the incoming flow quantity to two parts each part near a wall, as shown in Fig. 3, case 4.

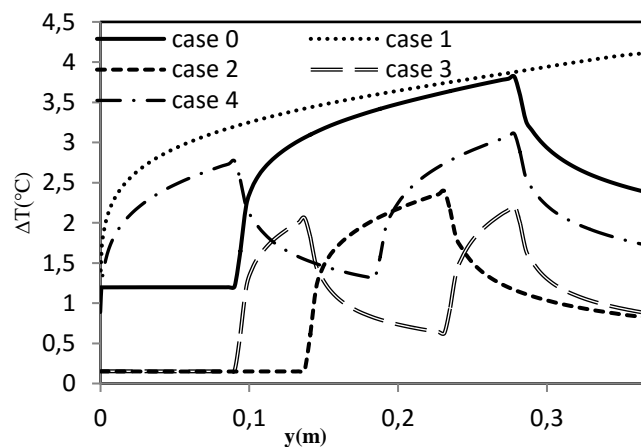


Figure 7: Vertical profiles of temperature in the heated plate for $Ra^*=4.5 \cdot 10^6$

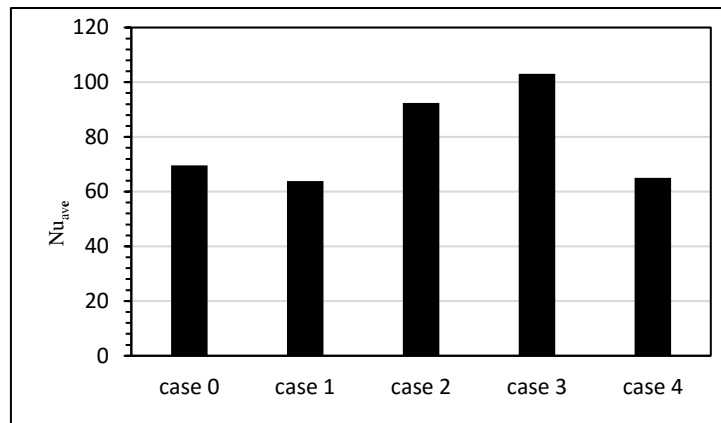


Figure 8: Average Nusselt number plots for all studied cases

6. Conclusion

The influence of length, number and alternation of heat sources on the heat transfer and flow characteristics in an asymmetrically heated channel has been investigated numerically. For modified Rayleigh number equal to 4.5×10^6 based on channel aspect ratio equal to 5.2 (for case0). Overall, the heat transfer and flow characteristics are strongly affected by the length, number and alternation of heat sources. The study leads to the following conclusions:

- A hydrodynamic boundary layer type flow in the vicinity of the heated wall is noticed for all studied cases.
- The length of the heated zone has a significant effect on the flow structure, i.e. the bigger is the length of the heated zone, the bigger the length of the revers flow is. Consequently, the lower the quantity of the entering fluid is. Large passage induces large quantity of the cold fluid coming from the channel inlet which leads to more heat extraction.
- The activation of the second hydrodynamic boundary layer along the right wall by the presence of the two separated heat sources on the second wall has a significant effect on the flow structure, especially on the revers flow which blocks the channel top-end. Allowing a significant quantity of the fluid to passes through the channel, albeit it is divided on to two parts, each part flowing adjacent to a wall.
- The largest heat transfer rate represented by Nu_{ave} is found for case 3 of value equal to 103,02. Which means the lower temperatures are found for the case 3, where the length of the heated zone is $\frac{1}{4}$ of the entire length of the channel wall.

References

- [1] D. Ospir, C. Popa, C. Chereches, G. Polidori, S. Fohanno, Flow visualization of Natural Convection in a Vertical Channel with Asymmetric heating, *International communications in Heat and Mass Transfert* 39 (2012) 486-493.
- [2] G. Polidori, S. Fatnassi, R. Ben Maad, S. Fohanno, F. Beaumont, Early-stage dynamics in the onset of free-convective reversal flow in an open-ended channel asymmetrically heated, *International Journal of Thermal Sciences* 88 (2015) 40-46.
- [3] S.V. Patankar, *Numerical Heat Transfer and Fluid Flow*, Hemisphere, Washington, DC, 1980.
- [4] C. Hemmer, C. V. Popa, A. Sergent, G. Polidori, Heat and fluid flow in an uneven heated chimney, *International Journal of Thermal Sciences* 107 (2016) 220-229.

- [5] W. Elenbaas, Heat dissipation of parallel plates by free convection, *Physica* 9 (1942) 1–28.
- [6] G. Desrayaud , E. Chénier, A. Joulin, A. Bastide, B. Brangeon , J.P. Caltagirone, Y. Cherif , R. Eymard , C. Garnier, S. Giroux-Julien, Y. Harnane, P. Joubert, N. Laaroussi, S. Lassue, P. Le Quéré, R. Li, D. Saury, A. Sergent, S. Xin, A. Zoubir, Benchmark solutions for natural convection flows in vertical channels submitted to different open boundary conditions, *International Journal of Thermal Sciences* 72 (2013) 18-33.
- [7] S. Fohanno, A. Tribech, C. Popa, G. Polidori, Simulation Expérimentale des modes de ventilation dans les parois double-peau, 21ème rencontres universitaire de genie Civil, Artes CD-ROM, La grande Motte (2006).
- [8] D. Ospir, C. Popa, C. Chereches, S. Fohanno, M. Chereches, Dynamique d'un Ecoulement de Convection Naturelle dans un Canal Vertical, 13^{ème} Congrès Français de Visualisation et de Traitement d'Images en Mécanique des Fluides, Reims,(2009).
- [9] D. Ospir, C. Popa, C. Chereches, G. Polidori, S. Fohanno, Flow visualization of Natural Convection in a Vertical Channel with Asymmetric heating, *International communications in Heat and Mass Transfert* 39 (2012) 486-493.
- [10] C. Popa, D. Ospir, S. Fohanno, C. Chereches, Numerical simulation of Dynamical Aspects of Natural Convection flow in a Double-Skin Façade, *Energy and Buildings* 50 (2012) 229–233.
- [11] F .Dupont, F.Ternat, S.Somat, R.Blondou, Two-dimension experimental study of the reverse flow in a free convection channel with active walls differentially heated, *Experimental Thermal and Fluid Science* 47 (2013) 150–157
- [12] G. Polidori, S. Fatnassi, R. Ben Maad, S. Fohanno, F. Beaumont, Early-stage dynamics in the onset of free-convective reversal flow in an open-ended channel asymmetrically heated, *International Journal of Thermal Sciences* 88 (2015) 40-46.
- [13] A. A. Imran, Jalal M. Jalil, Sabah T. Ahmed, Induced flow for ventilation and cooling by a solar chimney, *Renewable Energy* 78 (2015) 236e244.
- [14] C. Hemmer, A. Abidi-Saad, C. V. Popa, G. Polidori, Early development of unsteady convective laminar flow in an inclined channel using CFD: Application to PV panels, *Solar Energy* 146 (2017) 221–229.
- [15] C. Hemmer, C. V. Popa, A. Sergent, G. Polidori, Heat and fluid flow in an uneven heated chimney, *International Journal of Thermal Sciences* 107 (2016) 220-229.
- [16] O.A. Tkachenko, V. Timchenko, S. Giroux-Julien, C.Ménézo, J.H. Yeoh, J.A. Reizes, E. Sanvicente, M. Fossa, Numerical and experimental investigation of unsteady natural convection in a non-uniformly heated vertical open-ended channel, *International Journal of Thermal Sciences* 99 (2016) 9-25.
- [17] L.M. Candanedo, A. Athienitis, K. Park, Convective heat transfer coefficients in a building-integrated photovoltaic/thermal system, *Journal of Solar Energy Engineering* 133 (2011) 021002-1–021002-14.
- [18] A. Abidi-Saad, M. Kadja, C. Popa, G. Polidori, Effect of adiabatic square ribs on natural convection in an asymmetrically heated channel, *Heat Mass Transfer* (2017) 53: 743
- [19] A. Abidi-Saada, G. Polidori, M. Kadja, F. Beaumont, C. V. Popa, A. Korichi, Experimental investigation of natural convection in a vertical rib-roughened channel with asymmetric heating, *Mechanics Research Communications* Volume 76, September 2016, Pages 1–10